Photoexcitation and Charge-Transfer-to-Solvent Relaxation Dynamics of the I − (CH 3 CN) Complex

ARTICLE *in* THE JOURNAL OF PHYSICAL CHEMISTRY A · JULY 2013

Impact Factor: 2.69 · DOI: 10.1021/jp403586u · Source: PubMed

3 AUTHORS, INCLUDING:

Qadir K Timerghazin
Marquette University
50 PUBLICATIONS **370** CITATIONS

SEE PROFILE

THE JOURNAL OF PHYSICAL CHEMISTRY A

Article

pubs.acs.org/JPCA

Photoexcitation and Charge-Transfer-to-Solvent Relaxation Dynamics of the $I^-(CH_3CN)$ Complex

Chun C. Mak, Qadir K. Timerghazin,† and Gilles H. Peslherbe*

Centre for Research in Molecular Modeling (CERMM) and Department of Chemistry and Biochemistry, Concordia University, 7141 Sherbrooke Street West, Montréal, Québec, Canada H4B 1R6

ABSTRACT: Photoexcitation of iodide−acetonitrile clusters, $I^-(CH_3CN)_n$, to the charge-transfer-to-solvent (CTTS) state and subsequent cluster relaxation could result in the possible formation of cluster analogues of the bulk solvated electron. In this work, the relaxation process of the CTTS excited iodide−acetonitrile binary complex, $[I^-(CH_3CN)]^*$, is investigated using rigorous ab initio quantum chemistry calculations and direct-dynamics simulations to gain insight into the role and motion of iodine and acetonitrile in the relaxation of CTTS excited $I^-(CH_3CN)_n$. Computed potential energy curves and profiles of the excited electron vertical detachment energy for $[I^-(CH_3CN)]^*$ along the iodine−acetonitrile distance coordinate reveal for the first time significant dispersion effects between iodine and the excited electron, which can have a significant stabilizing effect on the latter. Results of direct-dynamics simulations demonstrate that $[I^-(CH_3CN)]^*$ undergoes dissociation to iodine and acetonitrile fragments, resulting in decreased stability of the excited electron. The present work provides strong evidence of solvent translational motion and iodine ejection as key aspects of the early time relaxation of CTTS excited $I^-(CH_3CN)_n$ that can also have a substantial impact on the subsequent electron solvation processes and further demonstrates that intricate details of the relaxation process of CTTS excited iodide−polar solvent molecule clusters make it heavily solvent-dependent.

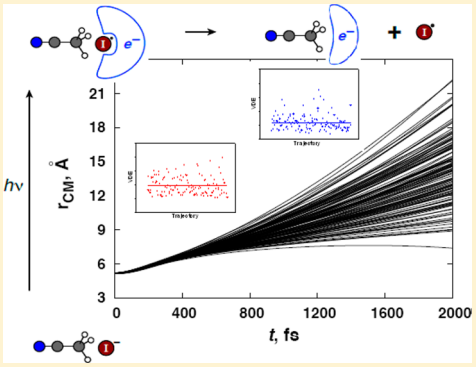

1. INTRODUCTION

Charge-transfer-to-solvent (CTTS) excited states constitute one of the most important features of the photochemistry of inorganic anions in polar solvent media.[1] Excitation to CTTS states involves the transfer of an excess electron from the anion to an orbital bound by the collective electric field of several solvent molecules. The bulk CTTS excited state is believed to be very similar in nature to the solvated electron, and in fact, the latter can be easily produced from the former.[2−4] The nature of the CTTS states has been a topic of long-standing interest from both experimentalists and theoreticians,[1] and the ultrafast excited electron and solvent dynamics following CTTS excitation has attracted considerable attention.[4−8] Whereas the gas-phase analogues of the solvated electron, that is, small solvent cluster anions, have been known for a few decades,[9] the CTTS precursor states in finite anion−solvent clusters were first observed much more recently.[10] Interestingly, just before the first experimental observations of CTTS states in clusters were reported,[11−13] Combariza et al. speculated, based on quantum chemistry calculations,[14] that CTTS states might potentially be observed only for very large halide−solvent clusters. However, Johnson and co-workers reported experimental observations of bound excited states just below the photodetachment threshold for a number of clusters formed by iodide and a few polar solvent molecules, including acetone, acetonitrile, and water: $I^-(CH_3COCH_3)$, $I^-(CH_3CN)_{1-2}$, and $I^-(H_2O)_{1-4}$.[11−13] By analogy to the bulk situation, where the relaxation of CTTS states leads to solvated electrons, the relaxation of the CTTS precursor states in clusters was found to produce solvent cluster anions with high yields.[11,12]

The relaxation of iodide−polar solvent clusters excited to the CTTS state, $[I^-(Solv)_n]^*$, has attracted considerable interest because the detailed molecular mechanism directly reflects the role of individual solvent molecules in the electron solvation process. In a series of femtosecond photoelectron spectroscopy experiments, Neumark and co-workers have investigated the relaxation of $[I^-(Solv)_n]^*$ (Solv = H_2O, NH_3, CH_3OH, CH_3CH_2OH, and CH_3CN), revealing the intriguing influence of the type of solvent on the electron solvation processes occurring during $[I^-(Solv)_n]^*$ relaxation.[15−23] Complementary theoretical work[24−35] has primarily focused on the electronic properties and dynamics of $[I^-(H_2O)_n]^*$ due to the importance of water as nature's most abundant and ubiquitous solvent, but recently, preliminary ab initio molecular dynamics simulations of $[I^-(CH_3OH)_n]^*$ have offered some important insights into the pronounced solvent dependence of the relaxation mechanism of $[I^-(Solv)_n]^*$.[36] While it has been shown unequivocally that $[I^-(H_2O)_n]^*$ undergoes dramatic reorganization of the water cluster moiety initiated by repulsive iodine−hydrogen interactions that leads ultimately to the stabilization of the excited electron,[35] $[I^-(CH_3OH)_n]^*$

Special Issue: Joel M. Bowman Festschrift

Received: April 11, 2013
Revised: June 28, 2013
Published: July 2, 2013

   dx.doi.org/10.1021/jp403586u | J. Phys. Chem. A 2013, 117, 7595−7605

relaxation on the other hand, which involves a much more complicated modulation of the excited electron stability, appears to involve multiple pathways characterized by dissociation to $I^{\bullet}$ and $(CH_3OH)_n^-$ and fragmentation of the solvent cluster moiety. These results highlight the central role of solvent−solvent and electron−solvent interactions in the electron solvation processes occurring in $[I^-(Solv)_n]^*$ and provide a rational explanation for the pronounced effect of solvent type on the nature of $[I^-(Solv)_n]^*$ relaxation pathways; more limited hydrogen-bonding in methanol clusters relative to water clusters facilitates fragmentation in $[I^-(CH_3OH)_n]^*$, thereby reducing the propensity for the excited electron to be trapped and stabilized in the solvent cluster relative to $[I^-(H_2O)_n]^*$.

While extensive experimental and theoretical work on the relaxation of $[I^-(H_2O)_n]^*$ and $[I^-(CH_3OH)_n]^*$ has led to important insights into the molecular basis of solvent-dependent electron solvation pathways in $[I^-(Solv)_n]^*$, $[I^-(CH_3CN)_n]^*$ have also attracted interest as they offer the opportunity to investigate the dynamics of a more "internalized" electron at the molecular level.[21] $I^-(CH_3CN)_n$ are believed to adopt "interior" solvation states,[37,38] in contrast to $I^-(H_2O)_n$ and $I^-(CH_3OH)_n$, in which iodide is primarily located at the cluster surface,[39−44] and as such, the excited electron in $[I^-(CH_3CN)_n]^*$ is also expected to be internalized, at least initially. Femtosecond photoelectron spectroscopy experiments performed on $[I^-(CH_3CN)_n]^*$ by Neumark and co-workers indicate that the excited electron vertical detachment energy (VDE) for $[I^-(CH_3CN)_n]^*$, which reflects the stability of the excited electron, decreases over several hundred femtoseconds by 0.10−0.35 eV before subsequently increasing by 0.30−0.45 eV over several picoseconds.[21] On the basis of limited earlier molecular dynamics simulations employing density functional theory,[45] the initial drop in the excited electron VDE was attributed to an expansion of the cavity occupied by the excited electron and the I atom formed in the excitation process, combined with possible localization of the excited electron on one or two acetonitrile molecules. The subsequent increase in the excited electron VDE could be attributed to contraction of the solvent cavity, along with possible iodine ejection, perhaps leading to the formation of an internally trapped electron. The proposed pathway remains speculative, however, and no conclusive insights into the detailed molecular motions involved in the relaxation and electron solvation process of $[I^-(CH_3CN)_n]^*$ have been obtained to date.

In this respect, $I^-(CH_3CN)_n$ (n = 1) lends itself as the simplest case for detailed computational studies of the photoexcitation process and CTTS excited-state dynamics of $I^-(CH_3CN)_n$, and in fact, recent photoelectron spectroscopy experiments performed on $I^-(CH_3CN)$ have highlighted the need for an in depth understanding of the dynamics and electron−molecule interactions involved in the process of electron detachment through CTTS states.[46] The small size and high symmetry of this binary complex also allow quantum chemistry calculations at relatively high levels of theory, which are very important for benchmarking various theoretical procedures that can be used for large-scale molecular dynamics simulations of larger $[I^-(CH_3CN)_n]^*$ clusters. In addition, with only one acetonitrile molecule, which alone possesses a sufficient dipole moment to trap an excess electron in a dipole-bound state, $[I^-(CH_3CN)]^*$ presents a unique opportunity to examine by itself the solvent molecular motion that is of paramount importance in the electron transfer and solvation dynamics of iodide−polar solvent molecule clusters. In fact, $(CH_3CN)^-$, the final product produced upon CTTS excitation of $I^-(CH_3CN)$,[12] is among the smallest systems with an excess electron trapped in a dipole-bound state, that is, one of the smallest cluster precursors of the solvated electron.

In the present article, we report high-level quantum chemistry calculations and ab initio molecular dynamics simulations of the CTTS state of the $I^-(CH_3CN)$ binary complex. The nature of the electronic transitions involved and various components of the excitation energy are revisited in detail, and the role of spin−orbit coupling (SOC) in the CTTS state of iodide−solvent clusters is examined for the first time. The potential energy profiles for the excited and ionized states are characterized using rigorous quantum chemistry calculations and are used to validate an inexpensive yet reliable computational procedure, which is subsequently used in realistic first-principles excited-state molecular dynamics simulations of $[I^-(CH_3CN)]^*$ relaxation. The outline of this article is as follows: the computational methods are outlined in section 2, the static picture of the photoionization and photoexcitation of $I^-(CH_3CN)$ is presented in section 3, the potential energy profiles of the excited and ionized states are discussed in section 4, the dynamics of the excited state are given in section 5, and concluding remarks follow in section 6.

2. COMPUTATIONAL METHODS

The structure of the $I^-(CH_3CN)$ complex was optimized, and its harmonic vibrational frequencies were calculated using second-order Møller−Plesset (MP2) perturbation theory.[47] The Dunning's correlation-consistent polarized double-ζ basis set augmented with diffuse functions (aug-cc-pVDZ) was used for the hydrogen, carbon, and nitrogen atoms,[48] and the relativistic large-core ECP46MDF pseudopotential and corresponding basis set by Stoll et al.[49] were used for the iodine atom. This basis set combination will be further referred to simply as the DZ basis set for brevity.

The excited and ionized states of the $I^-(CH_3CN)$ complex were calculated with multireference second-order perturbation theory (CASPT2)[50] with the state-averaged complete active space self-consistent field (CASSCF)[51,52] reference wave function. CASSCF calculations used a (6,4) active space consisting of the 3 occupied 5p orbitals of iodine and the lowest unoccupied orbital, resulting in 10 singlet configuration state functions (CSFs) and 6 triplet CSFs. A total of 10 states (4 singlet states, 3 triplet states, and 3 ionized states) were included in the state-averaging. For excited-state calculations, the DZ basis set was further augmented by 8 diffuse sp functions generated in an even-tempered manner from the average of the outermost s and p functions of the aug-cc-pVDZ basis set using the geometric progression ratio of 3.2,[53] resulting in an exponent of 1.9414×10^{-6} au for the most diffuse sp basis function. The augmented DZ basis set will be simply referred to as DZ+. In most calculations, the additional diffuse sp functions were centered on the methyl group carbon atom. In a number of calculations, the "floating center" technique[54] was used, with the position of the diffuse center optimized with CASPT2 using numerical gradients.

SOC calculations were performed with the interacting states method, using the effective one-electron spin−orbit (SO) operator included in the relativistic effective core potential of the iodine atom.[49] The CASPT2 energies of the lowest singlet and triplet electronic states were corrected on the basis of SOC

dx.doi.org/10.1021/jp403586u | J. Phys. Chem. A 2013, 117, 7595−7605

elements calculated using the CASSCF wave function. This approach is referred to as CASPT2-SOC.

In order to properly describe the excess electron VDEs of dipole-bound systems such as $[I^-(CH_3CN)]^*$, a higher-order treatment of electron correlation effects is required,[53,55−58] and as such, the excited electron VDEs of $[I^-(CH_3CN)]^*$ were computed with the coupled cluster method with single, double, and noniterative triple excitations [CCSD(T)] for open-shell systems.[59,60] In these calculations, the aug-cc-pVTZ basis set[48] was used for carbon, hydrogen, and nitrogen, while the ECP46MWB pseudopotential[61] and the corresponding triple-ζ basis set were used for iodine.[62] In addition, nine sets of diffuse functions were added to the carbon atom of the methyl group to describe the excited electron.[53] The exponents were generated in an even-tempered manner with a progression ratio of 3.2, beginning with the average of the outermost sp exponents of the aug-cc-pVTZ basis set. The four tightest sets of functions contained functions of s, p, and d symmetry, while the remaining sets of functions were of s and p symmetry, and the smallest exponent was 1.5×10^{-6} au. This basis set will hereafter be denoted TZ+.

Beginning with our early work on $I^-(H_2O)_n$ $(n = 3)$,[28] first-principles excited-state molecular dynamics simulations[63] have been used extensively to elucidate the CTTS excited-state relaxation of iodide−solvent clusters[31−36] as they paint a real-time dynamic picture that can be connected with state-of-the-art ultrafast photoelectron spectroscopy experiments. In this approach, the energy and atomic forces are calculated "on the fly" during the propagation of the atomic equations of motion by ab initio methods.[63] Unfortunately, molecular dynamics simulations employing high-level ab initio methods such as CASPT2 with large basis sets, which is used to compute the potential energy curves, are not yet feasible within the limits of current computational resources. Large-scale first-principles excited-state molecular dynamics simulations require a fast and robust model chemistry for which analytic energy gradients are readily available for efficient calculation of the forces.

In order to develop a suitable model chemistry for use in ab initio molecular dynamics simulations of $[I^-(CH_3CN)]^*$, two approaches were employed. The first approach was based on the "triplet approximation" for the calculation of CTTS states first employed by Bradforth and Jungwirth.[64] The triplet CTTS states are the lowest states of that multiplicity, and as such, single reference methods such as restricted open-shell Hartree−Fock (ROHF) theory and MP2 theory are appropriate for calculating the energies and forces of $[I^-(CH_3CN)]^*$. As will be shown below, the triplet states approximate the actual SO excited states of $[I^-(CH_3CN)]^*$ as well as the singlet states. In these calculations, the 6-31++G(d,p) basis set[65−67] was used for carbon, hydrogen, and nitrogen, while the effective core potential and corresponding valence basis set of Kurtz and co-workers were used for iodine.[68,69] This basis set was augmented with four s diffuse functions (exponents 0.012, 0.004, 0.00133, and 0.000444) on hydrogen and two sets of sp diffuse functions (exponents 0.008667 and 0.0009630) on iodine. This basis set will be referred to as Mid+. The second approach for modeling the excited state of $[I^-(CH_3CN)]^*$ involved the use of the configuration interaction with single excitations (CIS)[70] method. An economic double-ζ basis set referred to as Min+ was developed for use in these calculations. The Min+ basis set is constructed from the small double-ζ quality basis set of Mitin et al.[71] augmented by a diffuse s function for hydrogen and diffuse sp functions for carbon and nitrogen.[67] For iodine, the large-core effective core potential and corresponding basis set by Stevens et al.,[72] augmented by one diffuse sp shell,[73] was employed. To accommodate the dipole-bound electron, the basis set was further augmented by three additional diffuse sp shells centered on the carbon atom of the methyl group and two sp shells on the iodine atom. The diffuse exponents were generated from the outermost diffuse functions of the main basis set in an even-tempered manner using a geometric progression factor of 5.0.

Initial conditions for the excited-state molecular dynamics simulations were generated using the thermal Monte Carlo sampling technique[74] implemented in the VENUS reaction dynamics program[75] on the ground-state $I^-(CH_3CN)$ HF/Min + potential energy surface for $T = 150$ K. While there is a wide uncertainty about the actual temperature of $I^-(CH_3CN)_n$ clusters generated in experiments, this temperature estimate was obtained using Klots theory of the evaporative ensemble.[76] Then, 128 constant-energy trajectories were propagated using the dynamic reaction coordinate technique[77] employing the velocity Verlet algorithm,[63] as implemented in the GAMESS package,[78] with a time step of 0.3 fs for up to 2 ps.

In order to probe the effect of the relaxation process on the stability of the excited electron in $[I^-(CH_3CN)]^*$, the excited electron VDEs of the complex at the Franck−Condon geometry and at the end of the 2 ps relaxation process were computed with the CCSD(T)/TZ+ model chemistry as described above.

All CASSCF, CASPT2, and CCSD(T) calculations were performed with the MOLPRO package,[79] HF and MP2 calculations were performed with the MOLPRO and GAMESS[78] packages, and all CIS calculations were performed with GAMESS.

3. PHOTOEXCITATION AND PHOTOIONIZATION OF $I^-(CH_3CN)$

Figure 1 shows a general energetic scheme of photoionization and photoexcitation for iodide in the gas phase and in clusters.

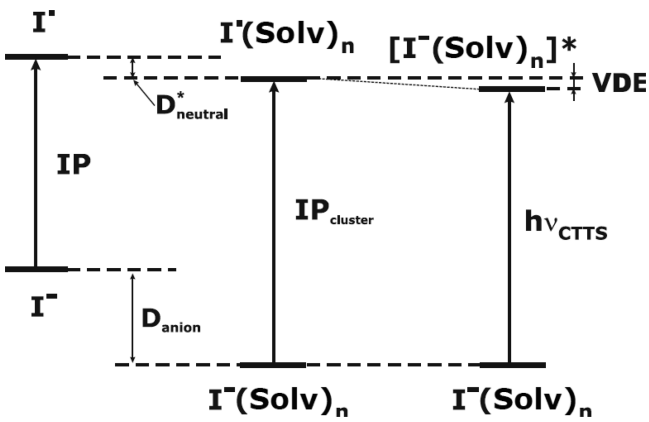

Figure 1. Photoionization and photoexcitation of free iodide and iodide−solvent clusters.

Free I^- does not possess bound excited states, and absorption of a photon with sufficient energy to overcome the ionization potential (IP) simply leads to photodetachment of the excess electron. Due to strong electrostatic and polarization interactions, complexation with one or more polar solvent molecules significantly stabilizes the ion (typically with anion binding energies D_{anion} larger than 10 kcal/mol or ~0.5 eV),

dx.doi.org/10.1021/jp403586u | J. Phys. Chem. A 2013, 117, 7595−7605

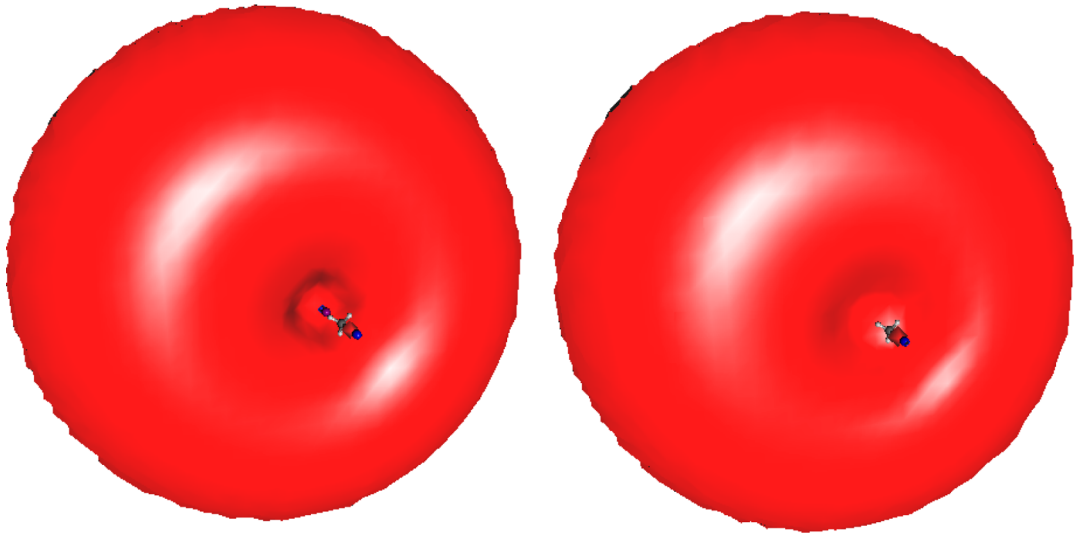

Figure 2. Distribution of the excited/excess electron in the excited iodide−acetonitrile complex and the dipole-bound acetonitrile anion (CASPT2/DZ+ natural orbitals; isosurfaces both enclose 45% of electron density).

Table 1. Calculated and Experimental Binding Energies and Other Properties Relevant to the Photoexcitation and Photoionization of the $I^-(CH_3CN)$ Complex[a]

	CASPT2/DZ+	CASPT2-SOC/DZ+	CCSD(T)/TZ+	expt.
$D_e[I^-(CH_3CN)]$	0.511	0.511	0.495	
$D_0[I^-(CH_3CN)]$	0.509[b]	0.509[b]	0.493[b]	0.494 ± 0.040[c]
$D_e^*[I^\bullet(CH_3CN)]$	0.032 (1^2E)	0.032 (I)	0.051 (1^2E)	
	0.021 (2^2A)	0.025 (II)		
		0.026 (III)		
$VDE[CH_3CN^-]$	11.0×10^{-3}		14.0×10^{-3}	$(11-18) \times 10^{-3}$[d]
$IP(I^-)$	2.979	2.674	3.17	3.059[e]
$IP[I^-(CH_3CN)]$	3.470 ($1^1A_1 \rightarrow 1^2E$)	3.165 (X → I)	3.67 ($1^1A_1 \rightarrow 1^2E$)	3.54, 4.48
	3.480 ($1^1A_1 \rightarrow 1^2A_1$)	3.171 (X → II)		
		4.084 (X → III)		
E_{CTTS}	3.463 ($1^1A_1 \rightarrow 1^1E$)	3.158 (X → I)	3.64 ($1^1A_1 \rightarrow 1^3E$)	3.53, 4.47
	3.474 ($1^1A_1 \rightarrow 2^1A_1$)	3.164 (X → II)		
		4.078 (X → III)		
$VDE[I^-(CH_3CN)]^*$	6.7×10^{-3} (1^1E)	7.0×10^{-3} (I)		≅10.0×10^{-3}
	5.9×10^{-3} (2^1A_1)	6.4×10^{-3} (II)		
	7.0×10^{-3} (1^3E)	6.7×10^{-3} (III)	2.5×10^{-2} (1^3E)	
	6.3×10^{-3} (1^3A_1)			

[a]All values in eV. [b]Zero-point energy-corrected value with vibrational frequencies calculated with MP2/DZ. [c]From ref 84. [d]From refs 85 and 12. [e]From ref 83.

whereas the stabilization by solvent molecules of the neutral iodine atom that forms upon photodetachment, $D^*_{neutral}$ is rather small. This differential solvation leads to the well-known increase of the IP of the solvated anion with an increasing number of solvent molecules in the cluster. If the solvent cluster possesses a dipole moment high enough ($\mu \geq 2.5$ D)[9] to bind the excess electron ejected from I^- upon photoexcitation, then a dipole-bound CTTS precursor excited state can be formed, slightly lower in energy than the photodetachment limit (Figure 1). Thus, the CTTS excitation energy is lower than the IP of iodide in the cluster ($IP_{cluster}$) by the excited electron VDE. In small clusters, this value is rather small (tens of meV), but the stabilization of the excited electron increases dramatically with cluster size, and the CTTS excitation energy can be significantly lower than the IP in larger clusters. Thus, in order to quantitatively reproduce experimentally observed CTTS excitation energies, one must be able to reproduce various energy components, including the IP of free iodide, the binding energies of iodide and neutral iodine to the solvent cluster, and, finally, the stabilization energy of the dipole-bound excited/excess electron to the solvent molecule(s).

As is immediately obvious from Figure 2, the excited electron distribution in the photoexcited iodide−acetonitrile complex is very similar to the excess electron distribution in the dipole-bound acetonitrile anion, in agreement with previous studies.[24,80]

Similarly to other intermolecular complexes formed by ^2P halogen atoms,[81,82] the interaction of the iodine atom formed upon photoionization/excitation of $I^-(CH_3CN)$ with the acetonitrile molecule gives rise to two possible electronic states that differ by the orientation of the half-filled 5p orbital relative to the C_3 axis of the CH_3CN molecule. In the lower, doubly degenerate 1^2E state, the half-filled p orbital of iodine is perpendicular to the C_3 axis and, in the 1^2A_1 state, the half-filled

dx.doi.org/10.1021/jp403586u | J. Phys. Chem. A 2013, 117, 7595−7605

p orbital is aligned along the symmetry axis (the singlet CTTS excited states are 1^1E and 2^1A_1, respectively). However, because the interaction of the iodine atom with the acetonitrile molecule is relatively weak and significantly smaller than the SOC constant of the free iodine atom (0.94 eV),[83] a typical Hund case (c) situation arises, and the value of the total spin is not a good quantum number to describe the ionized and excited states of iodide−solvent clusters. The SO mixing of the 1^1E and 2^1A_1 states of the excited complex gives rise to three SO states, labeled I, II, and III (X is used for the ground state of the $I^-(CH_3CN)$ complex, which is essentially the 1^1A_1 state); the first two states correlate with the $^2P_{3/2}$ limit of the free iodine atom, whereas the third one correlates with the $^2P_{1/2}$ limit.[81,82] For a complex with cylindrical symmetry, such as $Na^+\cdots I^\bullet$ or $I^\bullet(CH_3CN)$, one of the doubly degenerate states retains its character, whereas the other two SO states have mixed A_1 and E character. The spin quantum number is not a good quantum number for weak intermolecular complexes formed by iodine; therefore, the singlet and triplet CTTS states of iodide−solvent clusters are strongly mixed. As such, the lowest triplet excited state(s) can be as good of an approximation to the actual (SO) excited CTTS states as the first singlet state(s), further validating the triplet approximation approach proposed by Bradforth and Jungwirth to model the CTTS states in water clusters and in the bulk[64] and employed throughout this work with single-reference quantum chemistry methods [HF, MP2 or CCSD(T)] to model the CTTS states.

We now turn our attention to more quantitative aspects of the photoionization and photoexcitation of $I^-(CH_3CN)$. As we have demonstrated previously,[86] ab initio (MP2) calculations predict binding energies for the binary halide−acetonitrile clusters in excellent agreement with experimental data. Indeed, the binding energy of the $I^-(CH_3CN)$ complex calculated with CASPT2/DZ+ of 0.51 eV (11.74 kcal/mol) is well within the experimental range of 0.484 ± 0.040 eV (Table 1) and, furthermore, is in close agreement with the values obtained with the more rigorous CCSD(T)/TZ+ model chemistry. Interestingly, the iodide−acetonitrile complex is the only complex in the $X^-(CH_3CN)$ series (X = F, Cl, Br, I) to adopt a linear structure, resulting from sole ion−dipole interactions, while complexes formed with the other halides exhibit less symmetric, hydrogen-bonded minimum-energy structures.[86] The calculated binding energy of the iodine atom to an acetonitrile molecule in the equilibrium geometry of the parent $I^-(CH_3CN)$ cluster, D_e^*, is relatively small (0.02−0.03 eV or 0.5−0.7 kcal/mol with CASPT2/DZ+ and 0.051 eV or 1.2 kcal/mol with CCSD(T)/TZ+, Table 1). Thus, the shift of the IP of iodide upon complexation with acetonitrile is practically equal to the $I^-(CH_3CN)$ binding energy D_{anion} (Figure 1) and arises mainly from ground-state stabilization of iodide by the acetonitrile polar solvent molecule.

The quantum chemical treatment of systems with an extremely diffuse dipole-bound electron, such as the excited $I^-(CH_3CN)$ complex or the acetonitrile anion CH_3CN^-, is a challenging but well-understood problem.[9] The diffuse nature of the excited/excess electron dictates the use of extremely diffuse basis sets, which may cause severe convergence problems.[53] Dispersion interactions are also very important in the stabilization of the dipole-bound electron;[55−58] therefore, inclusion of dynamic electron correlation is necessary to produce reliable VDEs of the dipole-bound electron. Inspection of Table 1 suggests that both the CASPT2/DZ+ and CCSD(T)/TZ+ approaches provide an adequate description of the dipole-bound electron binding energy for the acetonitrile anion as they predict values in agreement with experiment and previously reported high-level ab initio quantum chemistry calculations.[58]

The IP of the free iodide anion is reproduced relatively well with both CASPT2/DZ+ and CCSD(T)/TZ+, although introduction of SOC leads to an underestimated value for the IP in the case of the CASPT2 calculations (by ca. 0.4 eV, Table 1). In fact, the IP of iodide (i.e., the electron affinity of iodine) is known to converge very slowly with basis set size, and even calculations employing the quintuple-ζ basis set aug-cc-pV5Z-PP still yield a slightly underestimated value.[87] Not surprisingly, the IP of the $I^-(CH_3CN)$ complex is also underestimated with CASPT2-SOC/DZ+ by almost 0.4 eV. The IP values uncorrected for SOC are closer to experimental data, most likely due to a cancellation of errors. Although the absolute value of the IP for the iodide−acetonitrile complex is reproduced poorly, the calculated shift of the IP between the free and complexed iodide (0.48−0.50 eV) is very close to the one observed in experimental studies (0.48 eV).[12] CASPT2-SOC/DZ+ calculations thus paint a correct quantitative picture of the photoexcitation and photoionization of the binary iodide−acetonitrile complex once the systematic error in the calculated IP of iodide is taken into account. The splitting between the 1^2E and 1^2A_1 ionized states of $I^-(CH_3CN)$ is small (∼0.01 eV), and it is even smaller for the two lowest SO states I and II, which may explain why it is not possible to distinguish them experimentally.[12]

Experimental data concerning the electron binding energy of the excited electron in the CTTS excited state of $I^-(CH_3CN)$ in the Franck−Condon region is rather uncertain, but photoneutral and photofragment action spectra suggest that the CTTS state lies ∼10 meV below the ionized states.[12] Our calculated results fall within the range of these values, with CASPT2/DZ+ predicting ionization energies of around 6−7 meV and CCSD(T)/TZ+ predicting a slightly larger value of 25 meV (Table 1). Not surprisingly, the triplet excited states are 0.3−0.4 meV more stable than the singlet states, and the SO mixing of the singlet and triplet E and A_1 states leads to slightly higher VDEs.

To summarize, CASPT2 and CASPT2-SOC ab initio quantum chemistry calculations with the highly diffuse DZ+ basis set provide a description of the photoionization and photoexcitation of $I^-(CH_3CN)$ in the Franck−Condon region in close agreement with experiment and higher-level electronic structure calculations. However, a complete understanding of the subsequent CTTS relaxation process requires information about extended regions of the excited-state potential energy surface, to which we now turn our attention.

4. POTENTIAL ENERGY CURVES FOR THE IONIZED AND EXCITED STATES OF $I^-(CH_3CN)$

Potential energy curves of the ionized and excited states of $I^-(CH_3CN)$ are important for understanding the relaxation and electron solvation pathways of $[I^-(CH_3CN)_n]^*$, and, computed with rigorous ab initio quantum chemistry methods, they may serve to benchmark the reliability of more efficient computational models for describing $[I^-(CH_3CN)]^*$ relaxation dynamics. Owing to the symmetry of $I^-(CH_3CN)$, it is relatively easy to map the potential energy surfaces of its ground, excited, and ionized states. Although the ground-state potential energy surface is known to be rather flat with respect to tilting of the iodide off of the acetonitrile C_3 symmetry axis

dx.doi.org/10.1021/jp403586u | J. Phys. Chem. A 2013, 117, 7595−7605

and the iodine is relatively free to float in the "methyl pocket" at nonzero temperatures,[86] the most relevant coordinate for ionized and excited-state relaxation dynamics is the C−I stretch coordinate along the C_3 axis (Figure 3). The rigidity of the

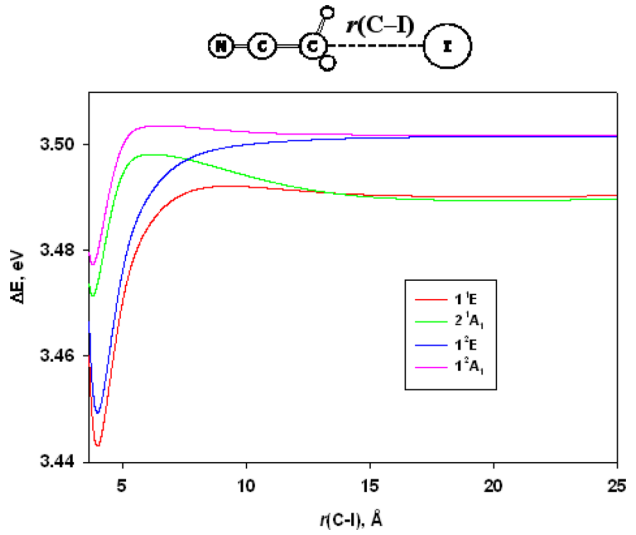

Figure 3. Potential energy curves (CASPT2/DZ+) for the non-SO-coupled singlet CTTS excited and doublet ionized states of the $I^-(CH_3CN)$ complex along the C−I stretch coordinate. The equilibrium ground-state energy of $I^-(CH_3CN)$ defines the energy reference, and the equilibrium C−I distance of $I^-(CH_3CN)$ corresponds to the onset of the curves.

acetonitrile molecule further simplifies the evaluation of the potential energy curves, in which the acetonitrile geometry is kept fixed and only the iodine−acetonitrile distance is varied. Figure 3 shows potential energy curves along the C−I stretch coordinate for the non-SO-coupled ionized and excited states of $I^-(CH_3CN)$, while Figure 4 shows potential energy curves for the SO states.

The potential energy curves for the 1^2E and 1^2A_1 states of $I^•(CH_3CN)$ have substantially different well depths due to the

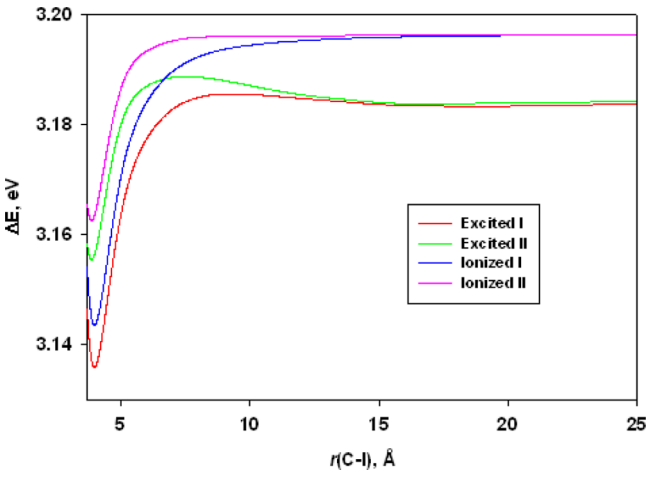

Figure 4. Potential energy curves (CASPT2-SOC/DZ+) for the lowest SO CTTS excited and ionized states of the $I^-(CH_3CN)$ complex along the C−I stretch coordinate. The equilibrium ground-state energy of $I^-(CH_3CN)$ defines the energy reference, and the equilibrium C−I distance of $I^-(CH_3CN)$ corresponds to the onset of the curves.

nonspherical distribution of the electron density of the iodine atom, giving rise to a nonzero quadrupole moment and relatively large differences in the polarizability along different axes.[82] In the lower 1^2E state, the interaction between acetonitrile and the iodine atom (located on the methyl group side) is relatively strong, with a potential well of ∼50 meV (∼1.2 kcal/mol) at a C−I distance of ∼4 Å (Figure 3). The well depth for the 1^2A_1 state is only 23 meV (∼0.5 kcal/mol), and the potential energy minimum is located at a shorter acetonitrile−iodine distance, with r(C−I) = 3.8 Å. The weaker stabilization of the 1^2A_1 state can be explained by the destabilizing interaction of the iodine atom quadrupole moment with the positive end of the acetonitrile molecular dipole and the lower polarizability of the iodine atom in the direction of the half-filled p orbital.

Generally, the potential energy curves for the CTTS excited states are similar to the corresponding ionized state curves but 5−12 meV lower in energy (Figure 3). However, the differences in the E−A_1 curves due to anisotropy are somehow amplified; unlike the 1^1E state, the 2^1A_1 state has a distinct maximum at a C−I distance of around 6 Å, which is ∼6 meV above the dissociation limit. The well depths for both singlet excited states, 45 and 16 meV (∼1.1 and ∼0.4 kcal/mol, respectively), are smaller than those for their ionized counterparts. The triplet excited states 1^3E and 1^3A_1 (not shown) are very similar to the singlet CTTS states, but they lie slightly lower by 1−1.5 meV.

Because the excited dipole-bound electron distribution may change significantly depending on the position of the iodine atom, the diffuse basis set centered on the methyl group carbon atom may become inadequate for some regions of the potential energy surface. Hence, potential energy curves were also evaluated with the "floating center" approach, where the position of the eight sp-diffuse functions used to describe the excited/excess electron was optimized at each point. The resulting potential energy curves are essentially the same as those shown in Figure 3.

Taking into account SOC does not significantly change the character of the potential energy curves for the ionized and excited states of $I^-(CH_3CN)$. The lower ionized and excited states (I) are practically identical to the corresponding 1^2E and $1^1E/1^3E$ states, respectively, and they are simply shifted down in energy by ∼0.3 eV because the I state has pure E parentage, similarly to other complexes of halogen atoms with cylindrical symmetry.[81,82] The II and III SO states (Figure 4, where only II is shown for clarity) have mixed E and A_1 character and therefore exhibit deeper energy wells than the corresponding non-SO states, with well depths of 33 and 29 meV (0.8 and 0.7 kcal/mol) for the ionized and excited states, respectively.

Figure 5 shows the distance profiles of the $[I^-(CH_3CN)]^*$ excited electron VDE computed with both CASPT2/DZ+ (for the non-SO-coupled singlet and triplet CTTS states, VDE profiles for the SO CTTS excited states are very similar and not shown) and CCSD(T)/TZ+ (for the 1^3E triplet CTTS state only). The CASPT2/DZ+ curves for the various CTTS states are all very similar and show that, for each state, the excited electron VDE increases by roughly 7 meV as the iodine−acetonitrile distance increases, reaching a maximum at r(C−I) ≈ 17 Å before decreasing by less than 1 meV to around 11 meV at larger r(C−I). These VDE profiles resemble those reported by Chen and Sheu for $[I^-(H_2O)_n]^*$[25] but appear qualitatively different from the CCSD(T)/TZ+ VDE profile. In the latter case, the excited electron VDE is highest at the ground-state

dx.doi.org/10.1021/jp403586u | J. Phys. Chem. A 2013, 117, 7595−7605

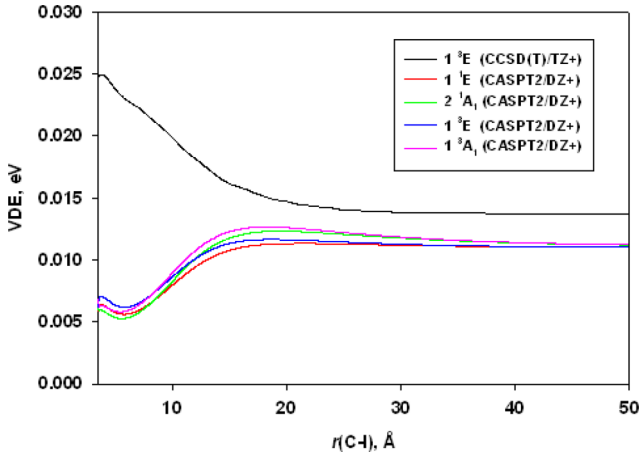

Figure 5. Excited electron VDEs for the singlet and triplet excited states of the $I^-(CH_3CN)$ complex along the C−I stretch coordinate.

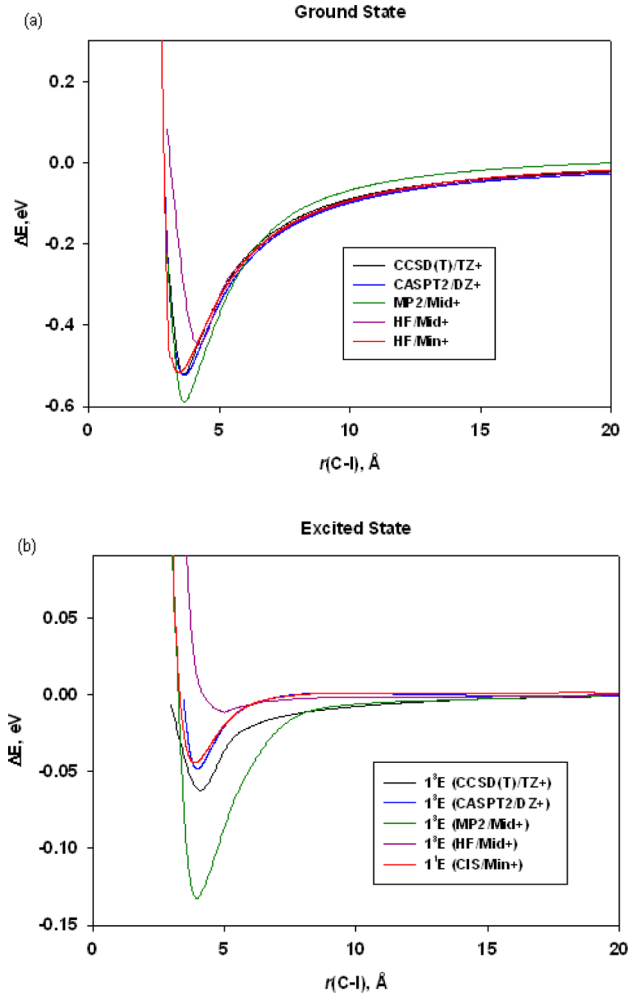

Figure 6. (a) Ground- and (b) excited-state potential energy curves of the $I^-(CH_3CN)$ complex computed with different model chemistries. Note that the vertical scale is different for the two plots. The asymptotic limit is set to zero for all curves.

equilibrium geometry of $I^-(CH_3CN)$ (25 meV) and decreases by around 10 meV as r(C−I) increases to 20 Å. Furthermore, CCSD(T)/TZ+ predicts a larger excited electron VDE for $[I^-(CH_3CN)]^*$ at all values of r(C−I). The discrepancies between the CASPT2/DZ+ and CCSD(T)/TZ+ VDE profiles appear to be due to the better treatment of dispersion effects between the diffuse excited electron and the electrons of the iodine atom by the second model chemistry. While exclusion effects have been invoked by Chen and Sheu to rationalize the destabilization of the excited electron distribution by the iodine atom in the case of $[I^-(H_2O)_n]^*$,[24,25] the present results suggest that more subtle dispersion interactions between the diffuse excited electron and the polarizable iodine atom, which can only be described with CCSD(T), appear to dominate. Indeed, higher-order electron correlation effects have been shown to contribute significantly to the stability of excess electrons in dipole-bound anions,[53,55−58] and the presence of the highly polarizable iodine atom in the region occupied by the excited electron distribution may make these effects even more important.

The stabilizing effect of the iodine atom on the excited electron distribution may at least partially account for the observed decrease of the excited electron VDE in $[I^-(Solv)_n]^*$ at long times as the iodine and solvent cluster depart from one another.[19,21,22] As shown earlier in the case of $[I^-(H_2O)_5]^*$,[35] separation of the excited electron distribution from the iodine atom is indeed a critical aspect of the relaxation process, but the subsequent electron solvation process was highly dependent on the solvent reorganization in that case. The shape of the potential energy curves for the excited states of $I^-(CH_3CN)$ and the associated profiles of the excited electron VDE indicate that separation of the iodine atom from the acetonitrile cluster moiety is also expected to contribute to the observed modulation of the stability of the excited electron in $[I^-(CH_3CN)_n]^*$; a detailed picture of the intricate molecular dynamics involved in the trapping of the excited electron can, however, only be obtained from accurate molecular dynamics simulations, the topic of the following section.

5. DYNAMICS OF PHOTOEXCITED $I^-(CH_3CN)$

Method Validation. Potential energy curves of the ground and excited states of $I^-(CH_3CN)$ computed with different model chemistries are shown in Figure 6. For ground-state $I^-(CH_3CN)$, the HF/Min+ potential energy curve is in close agreement with those computed with the more rigorous CASPT2/DZ+ and CCSD(T)/TZ+ model chemistries once it is shifted by −0.16 Å. On the other hand, HF/Mid+ underestimates the depth of the potential energy well by 0.07 eV (1.6 kcal/mol), while MP2/Mid+ overestimates it by a similar amount relative to the CASPT2/DZ+ or CCSD(T)/TZ+ curves. CIS also appears to provide a reasonable description of the excited state of $I^-(CH_3CN)$; the CIS and CASPT2 curves practically coincide once the CIS curves are shifted by r(C−I) = −0.16 Å. Relative to CCSD(T)/TZ+, however, CIS/Min+ slightly underestimates the depth of the potential energy well by 0.015 eV (0.35 kcal/mol), an amount that is not likely to have a significant impact on the nature of the excited-state dynamics given the amount of kinetic energy present in the system at 150 K (~0.3 eV). On the other hand, MP2/Mid+ overestimates the well-depth significantly by around 0.07 eV (1.6 kcal/mol), while HF/Mid+ underestimates it by a similar amount. Thus, the CIS/Min+ model chemistry was selected for use in the molecular dynamics simulations of the CTTS excited-state relaxation dynamics of $I^-(CH_3CN)$.

CTTS Relaxation Dynamics. The time evolution of the $[I^-(CH_3CN)]^*$ complex during CTTS relaxation and the fragment energy distributions at the end of the simulation time (2 ps) are shown in Figures 7 and 8, respectively. The

dx.doi.org/10.1021/jp403586u | J. Phys. Chem. A 2013, 117, 7595−7605

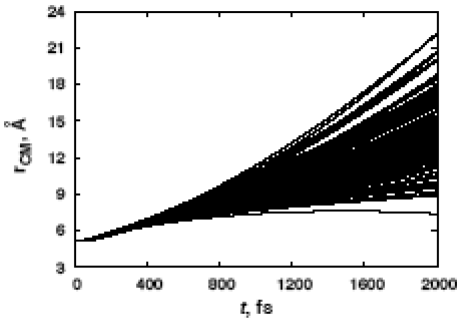

Figure 7. CTTS relaxation dynamics of the $I^-(CH_3CN)$ complex: evolution of the interfragment distance (measured as the distance between the fragment centers of mass, r_{CM}).

relaxation of $[I^-(CH_3CN)]^*$ is generally characterized by reasonably fast dissociation of the complex into $I^\bullet$ and CH_3CN^- fragments. By the end of the simulation time, the distance between iodine and acetonitrile is larger than 10 Å for most of the trajectories, the interfragment distance exceeds 20 Å for a few trajectories, and only one trajectory results in a complex loosely trapped in the excited-state potential energy well. These results are in good agreement with the experimental observation of the acetonitrile dipole-bound anion as the only negatively charged product of $[I^-(CH_3CN)]^*$ relaxation.[12]

Further insight into $[I^-(CH_3CN)_n]^*$ relaxation can be obtained by examining the final relative translational and rotational energies of the acetonitrile molecules (Figure 8a and b, respectively). Most of the trajectories result in acetonitrile molecules with moderate translational kinetic energy (0.5−3 kcal/mol), with a comparatively smaller number of trajectories resulting in acetonitrile molecules with high translational kinetic energy (up to 7 kcal/mol). The acetonitrile rotational energy, on the other hand, is negligible for more than half of the trajectories (Figure 8b), with dissociation predominantly proceeding by elongation of the iodine−acetonitrile distance along the C_3 axis of the complex, that is, along the coordinate of the potential energy curve in Figure 4, though a small number of trajectories lead to acetonitrile molecules with substantial rotational energy (~7 kcal/mol). These results tentatively suggest that translation of CH_3CN away from the iodine may dominate the initial relaxation of $[I^-(CH_3CN)_n]^*$, consistent with the hypothesis by Neumark and co-workers that the solvent cage surrounding iodine undergoes expansion in the early stages of the relaxation process.[21]

Comparison of the initial and final (after 2 ps) distributions of the $[I^-(CH_3CN)]^*$ excited electron VDEs obtained from the molecular dynamics simulations (Figure 9) provides important

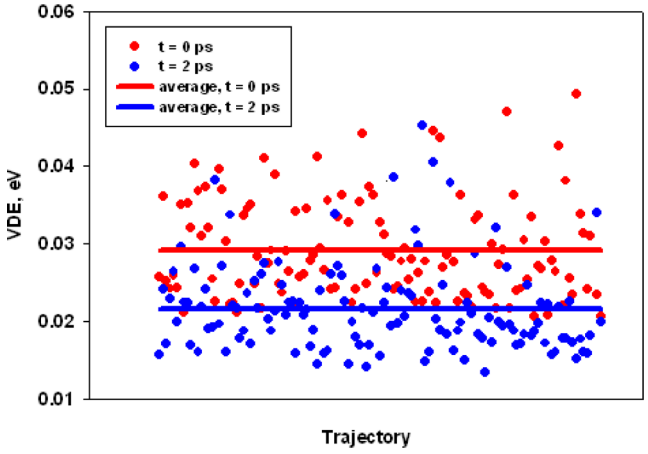

Figure 9. Scatter plot of the excited electron VDE of $[I^-(CH_3CN)]^*$ from the simulated trajectories, calculated with CCSD(T)/TZ+//CIS/Min+. Solid lines indicate the average VDE over 128 trajectories at each time.

insights into the influence of the relaxation process on the stability of the excited electron. Furthermore, because $I^-(CH_3CN)$ lacks the solvent network characteristic of larger $I^-(Solv)_n$, $[I^-(CH_3CN)]^*$ offers a unique opportunity to investigate the importance of iodine−solvent relative motion in the electron solvation process. At t = 0 ps, the excited electron VDEs of $[I^-(CH_3CN)]^*$ are distributed around an average value of 0.030 eV, although VDEs for individual starting configurations can vary widely. These VDE values are significantly larger than those at 2 ps, which are distributed around an average value of only 0.021 eV. These findings are not surprising in light of the nature of the CCSD(T)/TZ+ excited electron VDE profile of $[I^-(CH_3CN)]^*$ along the C−I stretch coordinate (Figure 5) and the overall tendency of the complex to dissociate along this coordinate as the relaxation proceeds (Figure 7). Even if translational motion seems to prevail in the relaxation process, rotation of the acetonitrile molecule may also have a significant impact on the excited electron VDE because the excited electron can move away from the region occupied by the iodine atom as it follows the rotating acetonitrile dipole, as in the early stages of

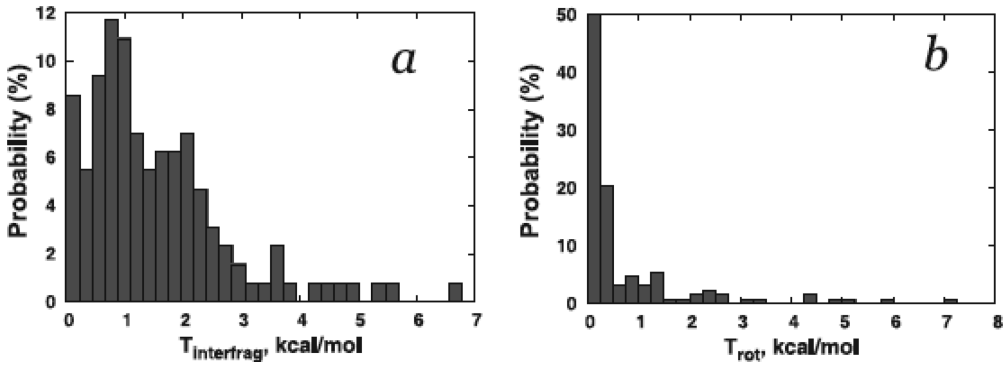

Figure 8. CTTS relaxation dynamics of the $I^-(CH_3CN)$ complex: interfragment relative kinetic energy T_{rel} (a) and rotational energy of the acetonitrile moiety T_{rot} (b). All energies are averaged over the last 75 fs of the simulation.

dx.doi.org/10.1021/jp403586u | J. Phys. Chem. A 2013, 117, 7595−7605

$[I^-(H_2O)_n]^*$[35] relaxation. Molecular translational motion is, however, expected to play a far greater role in $[I^-(CH_3CN)_n]^*$ relaxation and the corresponding modulation of the stability of the excited electron; this unique aspect of $[I^-(CH_3CN)_n]^*$ might be due to the high moment of inertia of acetonitrile compared with that of water and methanol and the resulting hindrance toward rotational excitation.

While substantial differences exist between $[I^-(CH_3CN)]^*$ and $[I^-(CH_3CN)_n]^*$ due to the absence of solvent−solvent interactions in the former complex, it is instructive to consider the simulated $[I^-(CH_3CN)]^*$ relaxation dynamics in the context of the recent femtosecond photoelectron spectroscopy experiments on $[I^-(CH_3CN)_n]^*$ performed by Neumark and co-workers.[21] These experiments indicate that, during the first ∼300 fs following excitation, the excited electron VDE of $[I^-(CH_3CN)_n]^*$ decreases substantially by 0.1−0.3 eV depending on the number of solvent molecules present, before increasing again by up to 0.45 eV over the next few picoseconds. While the average decrease in the simulated excited electron VDE of $[I^-(CH_3CN)]^*$ is an order of magnitude smaller, the present results indicate that translational motion of the solvent molecules is likely to reduce the attractive excited electron−iodine interactions and the associated VDE in the early stages of $[I^-(CH_3CN)_n]^*$ relaxation. Indeed, expansion of the solvent cage was observed in the preliminary molecular dynamics simulations of Takayanagi, in which a very limited number of trajectories were propagated from mostly local minimum-energy $I^-(CH_3CN)_n$ (n = 2,3) configurations.[45] The present results also highlight the possible contribution of rotational motion in the $[I^-(CH_3CN)_n]^*$ relaxation process; solvent rotation can not only modulate the excited electron−iodine interaction, but it can also assist in opening up the solvent "ring" surrounding iodine[44] in the Franck−Condon geometry of larger $[I^-(CH_3CN)_n]^*$ ($n \geq 5$), which would then facilitate the departure of iodine and the subsequent formation of the acetonitrile cluster anion with an internally solvated electron with higher VDE. Thus, while the present simulations of $[I^-(CH_3CN)]^*$ relaxation have provided some important insights into the types of solvent motion involved in the initial relaxation of $[I^-(CH_3CN)_n]^*$, extensive simulations of larger $[I^-(CH_3CN)_n]^*$ ($n \geq 2$) using the present approach may prove critical for understanding the unique aspects of CTTS relaxation leading to the formation of a possibly internally trapped electron in $[I^-(CH_3CN)_n]^*$.

6. CONCLUDING REMARKS

In this article, we report a detailed investigation of the CTTS photoexcitation and photoionization of the binary iodide−acetonitrile complex using high-level ab initio quantum chemistry methods. The ground, excited, and ionized states of the $I^-(CH_3CN)$ complex were characterized by CASSCF/CASPT2 calculations with a double-ζ quality basis set augmented by a large number of diffuse functions. Interestingly, only a small active space is necessary for these calculations for each state essentially possesses single-reference character. SOC was found to be so strong in this system that it heavily mixes the states, and as a result, the lowest triplet excited state(s) can be as good of an approximation to the actual (SO) excited CTTS states as the first singlet state(s), unambiguously validating for the first time the triplet approximation approach proposed by Bradforth and Jungwirth. Accordingly, very high level CCSD(T) calculations with an augmented triple-ζ quality basis set can be used to characterize the various states and paint an accurate picture of the photoexcitation and photoionization process.

These calculations indeed reproduce qualitative and quantitative aspects of the photoexcitation and photoionization of the $I^-(CH_3CN)$ complex in excellent agreement with available experimental data, thus providing solid ground for the computational investigation of the CTTS excited-state relaxation processes. To this end, potential energy curves for the ionized and CTTS excited states were calculated in order to unveil the dependence of the excited electron binding energy on the complex geometry. A stabilizing interaction between the iodine atom and the excited electron at short distance, which could influence the modulation of the excited electron VDE of $[I^-(CH_3CN)_n]^*$, was identified. An efficient two-level scheme for first-principles excited-state molecular dynamics simulations of the $I^-(CH_3CN)$ complex was developed, which makes use of a low-level economic model chemistry to propagate the equations of motion along the trajectories and high-level calculations to obtain the time profile of the excited electron VDE. Extensive simulations with realistic initial conditions were then performed of the CTTS relaxation dynamics of the iodide−acetonitrile complex. The present results highlight the importance of iodine detachment from the complex in the relaxation and electron solvation process of $[I^-(CH_3CN)_n]^*$, a critical aspect of the relaxation dynamics that appears to be shared with all $[I^-(Solv)_n]^*$.

AUTHOR INFORMATION

Present Address

[†]Q.K.T.: Department of Chemistry, Marquette University, P.O. Box 1881, Milwaukee, Wisconsin 53201-1881, United States.

Notes

The authors declare no competing financial interest.

ACKNOWLEDGMENTS

The authors would like to thank an anonymous reviewer for insightful comments. This work was funded by research grants from the Natural Sciences and Engineering Research Council (NSERC) of Canada. C.C.M. is the recipient of a Concordia University Doctoral Award of Excellence. Computational resources were provided by Calcul Québec and the Centre for Research in Molecular Modeling (CERMM).

REFERENCES

(1) Blandamer, M. J.; Fox, M. F. Theory and Applications of Charge-Transfer-to-Solvent Spectra. *Chem. Rev.* **1970**, *70*, 59−93.

(2) Jortner, J.; Levine, R.; Ottolenghi, M.; Stein, G. Photochemistry of the Iodide Ion in Aqueous Solution. *J. Phys. Chem.* **1961**, *65*, 1232−1238.

(3) Jortner, J.; Ottolenghi, M.; Stein, G. The Photochemistry of Aqueous Solutions of Chloride, Bromide, and Iodide Ions. *J. Phys. Chem.* **1964**, *68*, 247−255.

(4) Kloepfer, J. A.; Vilchiz, V. H.; Lenchenkov, V. A.; Germaine, A. C.; Bradforth, S. E. The Ejection Distribution of Solvated Electrons Generated by the One-Photon Photodetachment of Aqueous I^- and Two-Photon Ionization of the Solvent. *J. Chem. Phys.* **2000**, *113*, 6288−6307.

(5) Kloepfer, J. A.; Vilchiz, V. H.; Lenchenkov, V. A.; Bradforth, S. E. Femtosecond Dynamics of Photodetachment of the Iodide Anion in Solution: Resonant Excitation into the Charge-Transfer-to-Solvent State. *Chem. Phys. Lett.* **1998**, *298*, 120−128.

(6) Crowell, R. A.; Lian, R.; Shkrob, I. A.; Bartels, D. M.; Chen, X.; Bradforth, S. E. Ultrafast Dynamics for Electron Photodetachment from Aqueous Hydroxide. *J. Chem. Phys.* **2004**, *120*, 11712−11725.

(7) Martini, G. B.; Barthel, E. R.; Schwartz, B. J. Optical Control of Electrons During Electron Transfer. *Science* **2001**, *293*, 462−465.
(8) Martini, I. B.; Barthel, E. R.; Schwartz, B. J. Manipulating the Production and Recombination of Electrons During Electron Transfer: Femtosecond Control of the Charge-Transfer-to-Solvent (CTTS) Dynamics of the Sodium Anion. *J. Am. Chem. Soc.* **2002**, *124*, 7622−7634.
(9) Jordan, K. D.; Wang, F. Theory of Dipole-Bound Anions. *Annu. Rev. Phys. Chem.* **2003**, *54*, 367−396.
(10) Robertson, W. H.; Johnson, M. A. Molecular Aspects of Halide Ion Hydration: The Cluster Approach. *Annu. Rev. Phys. Chem.* **2003**, *54*, 173−213.
(11) Dessent, C. E., H.; Bailey, C. G.; Johnson, M. A. Observation of the Dipole-Bound Excited State of the I^--Acetone Ion−Molecule Complex. *J. Chem. Phys.* **1995**, *102*, 6335−6338.
(12) Dessent, C. E., H.; Bailey, C. G.; Johnson, M. A. Dipole Bound Excited States of the I^--CH_3CN and I^--$(CH_3CN)_2$ Ion−Molecule Complexes: Evidence for Asymmetric Solvation. *J. Chem. Phys.* **1995**, *103*, 2006−2015.
(13) Serxner, D.; Dessent, C. E., H.; Johnson, M. A. Precursor of the $I^-_{(aq)}$ Charge-Transfer-to-Solvent (CTTS) Band in I^--$(H_2O)_n$ Clusters. *J. Chem. Phys.* **1996**, *105*, 7231−7234.
(14) Combariza, J. E.; Kestner, N. R.; Jortner, J. Energy-Structure Relationships for Microscopic Solvation of Anions in Water Clusters. *J. Chem. Phys.* **1994**, *100*, 2865−70.
(15) Lehr, L.; Zanni, M. T.; Frischkorn, C.; Weinkauf, R.; Neumark, D. M. Electron Solvation in Finite Systems: Femtosecond Dynamics of Iodide·(Water)$_n$ Anion Clusters. *Science* **1999**, *284*, 635−638.
(16) Frischkorn, C.; Zanni, M. T.; Davis, A. V.; Neumark, D. M. Electron Solvation Dynamics in $I^-(NH_3)_n$ Clusters. *Faraday Discuss.* **2000**, *115*, 49−62.
(17) Davis, A. V.; Zanni, M. T.; Frischkorn, C.; Neumark, D. M. Time-Resolved Dynamics of Charge Transfer to Solvent States in Solvated Iodide Clusters. *J. Electron Spectrosc. Relat. Phenom.* **2000**, *108*, 203−211.
(18) Davis, A. V.; Zanni, M. T.; Weinkauf, R.; Neumark, D. M. Comment on 'Iodine Effect on the Relaxation Pathway of Photo-excited $I^-(H_2O)_n$ Clusters' [Chem. Phys. Lett. 335 (2001) 475]. *Chem. Phys. Lett.* **2002**, *353*, 455−458.
(19) Kammrath, A.; Verlet, J. R. R.; Bragg, A. E.; Griffin, G. B.; Neumark, D. M. Dynamics of Charge-Transfer-to-Solvent Precursor States in I^-(Water)$_n$ (n = 3−10) Clusters Studied with Photoelectron Imaging. *J. Phys. Chem. A* **2005**, *109*, 11475−11483.
(20) Verlet, J. R. R.; Kammrath, A.; Griffin, G. B.; Neumark, D. M. Electron Solvation in Water Clusters Following Charge Transfer from Iodide. *J. Chem. Phys.* **2005**, *123*, 231102/1−231102/4.
(21) Ehrler, O. T.; Griffin, G. B.; Young, R. M.; Neumark, D. M. Photoinduced Electron Transfer and Solvation in Iodide-Doped Acetonitrile Clusters. *J. Phys. Chem. B* **2009**, *113*, 4031−4037.
(22) Young, R. M.; Yandell, M. A.; Neumark, D. M. Dynamics of Electron Solvation in $I^-(CH_3OH)_n$ Clusters ($4 \le n \le 11$). *J. Chem. Phys.* **2011**, *134*, 124311/1−124311/10.
(23) Yandell, M. A.; Young, R. M.; King, S. B.; Neumark, D. M. Effects of Excitation Energy on the Autodetachment Lifetimes of Small Iodide-Doped ROH Clusters (R = H−, CH_3−, CH_3CH_2−). *J. Phys. Chem. A* **2012**, *116*, 2750−2757.
(24) Chen, H.-Y.; Sheu, W.-S. Precursors of the CTTS States in $I^-(H_2O)_n$ Clusters. *J. Am. Chem. Soc.* **2000**, *122*, 7534−7542.
(25) Chen, H.-Y.; Sheu, W.-S. Iodine Effect on the Relaxation Pathway of Photoexcited $I^-(H_2O)_n$ Clusters. *Chem. Phys. Lett.* **2001**, *335*, 475−480.
(26) Chen, H.-Y.; Sheu, W.-S. Reply to the Comment on 'Iodine Effect on the Relaxation Pathway of Photoexcited $I^-(H_2O)_n$ Clusters' [Chem. Phys. Lett. 335 (2001) 475]. *Chem. Phys. Lett.* **2002**, *353*, 459−462.
(27) Vila, F. D.; Jordan, K. D. Theoretical Study of the Dipole-Bound Excited States of $I^-(H_2O)_4$. *J. Phys. Chem. A* **2002**, *106*, 1391−1397.
(28) Timerghazin, Q. K.; Peslherbe, G. H. Further Insight into the Relaxation Dynamics of Photoexcited $I^-(H_2O)_n$ Clusters. *J. Am. Chem. Soc.* **2003**, *125*, 9904−9905.
(29) Lee, H. M.; Suh, S. B.; Kim, K. S. Solvent Rearrangement for an Excited Electron of $I^-(H_2O)_6$: Analog to Structural Rearrangement of $e^-(H_2O)_6$. *J. Chem. Phys.* **2003**, *119*, 7685−7692.
(30) Lee, H. M.; Kim, K. S. Solvent Rearrangement for an Excited Electron of the Iodide−Water Pentamer. *Mol. Phys.* **2004**, *102*, 2485−2489.
(31) Kolaski, M.; Lee, H. M.; Pak, C.; Dupuis, M.; Kim, K. S. Ab Initio Molecular Dynamics Simulations of an Excited State of $X^-(H_2O)_3$ (X = Cl, I) Complex. *J. Phys. Chem. A* **2005**, *109*, 9419−9423.
(32) Takayanagi, T.; Takahashi, K. Direct Dynamics Simulations of Photoexcited Charge-Transfer-to-Solvent States of the $I^-(H_2O)_6$ Cluster. *Chem. Phys. Lett.* **2006**, *431*, 28−33.
(33) Takahashi, K.; Takayanagi, T. Direct Dynamics Simulations of Photoexcited Charge-Transfer-to-Solvent States of the $I^-(H_2O)_n$ (n = 4, 5 and 6) Clusters. *Chem. Phys.* **2007**, *342*, 95−106.
(34) Kolaski, M.; Lee, H. M.; Pak, C.; Kim, K. S. Charge-Transfer-to-Solvent-Driven Dissolution Dynamics of $I^-(H_2O)_{2-5}$ Upon Excitation: Excited-State Ab Initio Molecular Dynamics Simulations. *J. Am. Chem. Soc.* **2008**, *130*, 103−112.
(35) Mak, C. C.; Timerghazin, Q. K.; Peslherbe, G. H. Photoinduced Electron Transfer and Solvation Dynamics in Aqueous Clusters: Comparison of the Photoexcited Iodide−Water Pentamer and the Water Pentamer Anion. *Phys. Chem. Chem. Phys.* **2012**, *14*, 6257−6265.
(36) Mak, C. C. Relaxation Pathways of Photoexcited Iodide−Methanol Clusters: Insights from Ab Initio Molecular Dynamics Simulations. *J. Phys. Chem. Lett.* **2013**, Submitted.
(37) Nguyen, T.-N. V.; Peslherbe, G. H. Microsolvation of Alkali and Halide Ions in Acetonitrile Clusters. *J. Phys. Chem. A* **2003**, *107*, 1540−1550.
(38) Nguyen, T.-N. V.; Hughes, S. R.; Peslherbe, G. H. Micro-solvation of the Sodium and Iodide Ions and Their Ion Pair in Acetonitrile Clusters: A Theoretical Study. *J. Phys. Chem. B* **2008**, *112*, 621−635.
(39) Koch, D. M.; Peslherbe, G. H. On the Transition from Surface to Interior Solvation in Iodide−Water Clusters. *Chem. Phys. Lett.* **2002**, *359*, 381−389.
(40) Robertson, W. H.; Karapetian, K.; Ayotte, P.; Jordan, K. D.; Johnson, M. A. Infrared Predissociation Spectroscopy of $I^-\cdot(CH_3OH)_n$, n = 1,2: Cooperativity in Asymmetric Solvation. *J. Chem. Phys.* **2002**, *116*, 4853−4857.
(41) Cabarcos, O. M.; Weinheimer, C. J.; Martinez, T. J.; Lisy, J. M. The Solvation of Chloride by Methanol−Surface versus Interior Cluster Ion States. *J. Chem. Phys.* **1999**, *110*, 9516−9526.
(42) Corbett, C. A.; Martinez, T. J.; Lisy, J. M. Solvation of the Fluoride Anion by Methanol. *J. Phys. Chem. A* **2002**, *106*, 10015−10021.
(43) Beck, J. P.; Lisy, J. M. Cooperatively Enhanced Ionic Hydrogen Bonds in $Cl^-(CH_3OH)_{1-3}$ Clusters. *J. Phys. Chem. A* **2010**, *114*, 10011−10015.
(44) Ayala, R.; Martinez, J. M.; Pappalardo, R. R.; Sanchez Marcos, E. Theoretical Study of the Microsolvation of the Bromide Anion in Water, Methanol, and Acetonitrile: Ion−Solvent vs Solvent−Solvent Interactions. *J. Phys. Chem. A* **2000**, *104*, 2799−2807.
(45) Takayanagi, T. Dynamical Calculations of Charge-Transfer-to-Solvent Excited States of Small $I^-(CH_3CN)_n$ Clusters. *J. Phys. Chem. A* **2006**, *110*, 7011−7018.
(46) Mbaiwa, F.; Wei, J.; Van Duzor, M.; Mabbs, R. Threshold Effects in I^-CH_3CN and I^-H_2O Cluster Anion Detachment: The Angular Distribution as an Indicator of Electronic Autodetachment. *J. Chem. Phys.* **2010**, *132*, 134304/1−134304/9.
(47) Hehre, W. J.; Radom, L.; Schleyer, P. v. R.; Pople, J. A. *Ab Initio Molecular Orbital Theory*; John Wiley and Sons: New York, 1985; p 548.

(48) Dunning, T. H., Jr. Gaussian Basis Sets for Use in Correlated Molecular Calculations. I. The Atoms Boron through Neon and Hydrogen. *J. Chem. Phys.* **1989**, *90*, 1007−1023.
(49) Stoll, H.; Metz, B.; Dolg, B. Relativistic Energy-Consistent Pseudopotentials — Recent Developments. *J. Comput. Chem.* **2002**, *23*, 767−778.
(50) Werner, H.-J. Third-Order Multireference Perturbation Theory The CASPT3 Method. *Mol. Phys.* **1996**, *89*, 645−661.
(51) Knowles, P. J.; Werner, H. J. An Efficient Second-Order MCSCF Method for Long Configuration Expansions. *Chem. Phys. Lett.* **1985**, *115*, 259−267.
(52) Werner, H. J.; Knowles, P. J. A Second Order Multiconfiguration SCF Procedure with Optimum Convergence. *J. Chem. Phys.* **1985**, *82*, 5053−5063.
(53) Skurski, P.; Gutowski, M.; Simons, J. How to Choose a One-Electron Basis Set to Reliably Describe a Dipole-Bound Anion. *Int. J. Quantum Chem.* **2000**, *80*, 1024−1038.
(54) Alfonso, D. R.; Jordan, K. D. Rearrangement Pathways of the Water Trimer and Tetramer Anions. *J. Chem. Phys.* **2002**, *116*, 3612−3616.
(55) Gutowski, M.; Skurski, P.; Boldyrev, A. I.; Simons, J.; Jordan, K. D. Contribution of Electron Correlation to the Stability of Dipole-Bound Anionic States. *Phys. Rev. A* **1996**, *54*, 1906−1909.
(56) Gutowski, M.; Skurski, P. Theoretical Study of the Dipole-Bound Anion $(HF)_2$. *J. Chem. Phys.* **1997**, *107*, 2968−2973.
(57) Gutowski, M.; Skurski, P. Dispersion Stabilization of Solvated Electrons and Dipole-Bound Anions. *J. Phys. Chem. B* **1997**, *101*, 9143−9146.
(58) Gutowski, M.; Jordan, K. D.; Skurski, P. Electronic Structure of Dipole-Bound Anions. *J. Phys. Chem. A* **1998**, *102*, 2624−2633.
(59) Knowles, P. J.; Hampel, C.; Werner, H.-J. Coupled Cluster Theory for High Spin, Open Shell Reference Wave Functions. *J. Chem. Phys.* **1993**, *99*, 5219−5227.
(60) Knowles, P. J.; Hampel, C.; Werner, H.-J. Erratum: "Coupled Cluster Theory for High Spin, Open Shell Reference Wave Functions" [*J. Chem. Phys.* 5219 (1993)]. *J. Chem. Phys.* **2000**, *112*, 3106−3107.
(61) Bergner, A.; Dolg, M.; Kuechle, W.; Stoll, H.; Preuss, H. Ab Initio Energy-Adjusted Pseudopotentials for Elements of Groups 13−17. *Mol. Phys.* **1993**, *80*, 1431−1441.
(62) Martin, J. M. L.; Sundermann, A. Correlation Consistent Valence Basis Sets for Use with the Stuttgart−Dresden−Bonn Relativistic Effective Core Potentials: The Atoms Ga−Kr and In−Xe. *J. Chem. Phys.* **2001**, *114*, 3408−3420.
(63) Bolton, K.; Hase, W. L.; Peslherbe, G. H. Direct Dynamics Simulations of Reactive Systems. In *Multidimensional Molecular Dynamics Methods*; Thompson, D. L., Ed.; World Scientific Publishing Co.: River Edge, NJ, 1998.
(64) Bradforth, S. E.; Jungwirth, P. Excited States of Iodide Anions in Water: A Comparison of the Electronic Structure in Clusters and in Bulk Solution. *J. Phys. Chem. A* **2002**, *106*, 1286−1298.
(65) Hehre, W. J.; Ditchfield, R.; Pople, J. A. Self-Consistent Molecular Orbital Methods. XII. Further Extensions of Gaussian-Type Basis Sets for Use in Molecular Orbital Studies of Organic Molecules. *J. Chem. Phys.* **1972**, *56*, 2257−2261.
(66) Hariharan, P. C.; Pople, J. A. The Influence of Polarization Functions on Molecular Orbital Hydrogenation Energies. *Theor. Chim. Acta* **1973**, *28*, 213−222.
(67) Clark, T.; Chandrasekhar, J.; Spitznagel, G. W.; Schleyer, P. V. R. Efficient Diffuse Function-Augmented Basis Sets for Anion Calculations. III. The 3-21+G Basis Set for First-Row Elements, Li−F. *J. Comput. Chem.* **1983**, *4*, 294−301.
(68) Labello, N. P.; Ferreira, A. M.; Kurtz, H. A. An Augmented Effective Core Potential Basis Set for the Calculation of Molecular Polarizabilities. *J. Comput. Chem.* **2005**, *26*, 1464−1471.
(69) Labello, N. P.; Ferreira, A. M.; Kurtz, H. A. Correlated, Relativistic, and Basis Set Limit Molecular Polarizability Calculations to Evaluate an Augmented Effective Core Potential Basis Set. *Int. J. Quantum Chem.* **2006**, *106*, 3140−3148.
(70) Foresman, J. B.; Head-Gordon, M.; Pople, J. A.; Frisch, M. J. Toward a Systematic Molecular Orbital Theory for Excited States. *J. Phys. Chem.* **1992**, *96*, 135−149.
(71) Mitin, A. V.; Hirsch, G.; Buenker, R. J. Accurate Small Split-Valence 3-21sp and 4-22sp Basis Sets for the First-Row Atoms. *Chem. Phys. Lett.* **1996**, *259*, 151−158.
(72) Stevens, W. J.; Krauss, M.; Basch, H.; Jasien, P. G. Relativistic Compact Effective Potentials and Efficient, Shared-Exponent Basis-Sets for the 3rd-Row, 4th-Row, and 5th-Row Atoms. *Can. J. Chem.* **1992**, *70*, 612−630.
(73) Check, C. E.; Faust, T. O.; Bailey, J. M.; Wright, B. J.; Gilbert, T. M.; Sunderlin, L. S. Addition of Polarization and Diffuse Functions to the LANL2DZ Basis Set for P-Block Elements. *J. Phys. Chem. A* **2001**, *105*, 8111−8116.
(74) Peslherbe, G. H.; Wang, H. B.; Hase, W. L. Monte Carlo Sampling for Classical Trajectory Simulations. *Monte Carlo Methods in Chemical Physics*; John Wiley & Sons: New York, 1999; Vol. *105*, pp 171−201.
(75) Hase, W. L.; Duchovic, R. J.; Hu, X.; Komornicki, A.; Lim, K.; Lu, D.; Peslherbe, G. H.; Swamy, K. N.; Van de Linde, S. R.; Wang, H.; Wolf, R. J. Venus, A General Chemical Dynamics Computer Program. *QCPE* **1996**, *16*, 671.
(76) Klots, C. E. Temperature of Evaporating Clusters. *Nature* **1987**, *327*, 222−223.
(77) Stewart, J. J. P.; Davis, L. P.; Burggraf, L. W. Semi-Empirical Calculations of Molecular Trajectories: Method and Applications to Some Simple Molecular Systems. *J. Comput. Chem.* **1987**, *8*, 1117−1123.
(78) Schmidt, M. W.; Baldridge, K. K.; Boatz, J. A.; Elbert, S. T.; Gordon, M. S.; Jensen, J. H.; Koseki, S.; Matsunaga, N.; Nguyen, K. A. General Atomic and Molecular Electronic Structure System. *J. Comput. Chem.* **1993**, *14*, 1347−1363.
(79) Werner, H.-J.; Knowles, P. J.; Knizia, G.; Manby, F. R.; Schütz, M.; et al. *Molpro*, version 2010.1, a Package of Ab Initio Programs. http://www.molpro.net (2012).
(80) Timerghazin, Q. K.; Peslherbe, G. H. Theoretical Investigation of Charge Transfer to Solvent in Photoexcited Iodide−Acetonitrile Clusters. *Chem. Phys. Lett.* **2002**, *354*, 31−37.
(81) Sanov, A.; Faeder, J.; Parson, R.; Lineberger, W. C. Spin−Orbit Coupling in $I{\cdot}CO_2$ and I·OCS Van Der Waals Complexes: Beyond the Pseudo-Diatomic Approximation. *Chem. Phys. Lett.* **1999**, *313*, 812−819.
(82) Timerghazin, Q. K.; Koch, D. M.; Peslherbe, G. H. Accurate Ab Initio Potential for the $Na^+{\cdot}I$ Complex. *J. Chem. Phys.* **2006**, *124*, 014313/1−014313/10.
(83) Sansonetti, J. E.; Martin, W. C. *Handbook of Basic Atomic Spectroscopic Data*; National Institute of Standards and Technology: Gaithersburg, MD, 2005; http://physics.nist.gov/physrefdata/handbook/index.html.
(84) Meot-Ner (Mautner), M. M.; Lias, S. G. Binding Energies between Ions and Molecules, and the Thermochemistry of Cluster Ions. In *Nist Chemistry Webbook*, Nist Standard Reference Database Number 69; Linstrom, P. J., Mallard, W. G., Eds.; National Institute of Standards and Technology: Gaithersburg MD, 2003; http://webbook.nist.gov.
(85) Desfrancois, C.; Abdoulcarime, H.; Khelifa, N.; Schermann, J. P. From 1/r to $1/r^2$ Potentials — Electron-Exchange between Rydberg Atoms and Polar-Molecules. *Phys. Rev. Lett.* **1994**, *73*, 2436−2439.
(86) Timerghazin, Q. K. Structure, Photochemistry and Charge-Transfer-to-Solvent Relaxation Dynamics of Anionic Clusters. Concordia University: Montréal, QC, 2006.
(87) Peterson, K. A.; Figgen, D.; Goll, E.; Stoll, H.; Dolg, M. Systematically Convergent Basis Sets with Relativistic Pseudopotentials. II. Small-Core Pseudopotentials and Correlation Consistent Basis Sets for the Post-D Group 16−18 Elements. *J. Chem. Phys.* **2003**, *119*, 11113−11123.